

**Development and Acaricide Toxicity of Abamectin as A Nanoemulsion Formulation  
Against The Red Palm Mite *Raoiella indicas***

**Naser H. Aldosary\* Ihab A. Alnajim Muhammad A. Al-Darwish**

**Date Palm Research Centre- University of Basrah, Basrah- IRAQ**

\*[naser.mohammed@uobasrah.edu.iq](mailto:naser.mohammed@uobasrah.edu.iq)

**Abstract**

The red palm mite (RPM) *Raoiella indica* is one of the common pests infesting date palms and may cause economic damage if left uncontrolled. Among the most widely used acaricides for controlling RPM is abamectin; however, the application of large quantities causes environmental damages. Due to the unique properties of nano-pesticides, the current study was designed to create a stable nanoemulsion of Abamectin via low-energy methods to control RPM. Eight hydrophilic-lipophilic balances (HLB) were prepared by blending different ratios of Tween 80 and Span 80 that were mixed with paraffin oil and water. HLB 9 and 11 combinations achieved homogeneity and one phase therefore two ternary phase diagrams were created, four pre-formulation points were selected, and 35 % v/v of Abamectin was uploaded to them. Two formulations passed kinetic and thermal stability. The formulations were nanoemulsion at 54.20 and 137.45 nm with good physical characterizations. The Abamectin nanoemulsion formulations recorded the largest droplet spreading and achieved high acaricidal toxicity after spray applications against RPM compared to the normal Abamectin formulation. These findings suggest that nanoformulations of Abamectin offer the potential to increase PRM control efficiency, which can reduce costs, delay the emergence of insect resistance, and reduce side effects.

**Keywords:** Abamectin, particle size, toxicity, spreading area, HLB.

## Introduction

The red palm mite (RPM), *Raoiella indica* Hirst (Acari: Tenuipalpidae), is one of the most pests that cause damage to fruit-producing trees. It is a common pest and can cause serious economic damage to numerous species of *Arecaceae*, especially the date palm (*Phoenix dactylifera*) and coconut (*Cocos nucifera* L.), as well as banana trees in various regions of the world (Vásquez et al., 2008; Nusantara et al., 2017). It is an oriental pest in origin, but the widespread prevalence in tropical and subtropical areas of this pest made it a severe problem (Welbourn, 2006; Zouba & Raeesi, 2010). Accordingly, Iraq, Iran, Pakistan, Mauritius, India, Oman, Russia, Sudan, and Egypt are the most prevalent countries of red mites (Welbourn, 2006; Zouba & Raeesi, 2010). Significant economic losses are caused by absorbing the leaves' sap through the stomata of the leaf by the adults and nymphs of RPM. The infestation symptoms appear as dispersed yellow spots, sharp yellowish colouration on the leaf or discolouration of the whole leaf. In severe infestations, the damage to young trees becomes more powerful than the old ones (Cocco et al., 2009; Pena et al., 2012). Several methods are applied to control RPM; however, chemical control is considered the most common strategy to manage the damage of this pest (Welbourn, 2006; Correa-Mendez et al., 2018). Some natural acaricides, such as Abamectin were approved under laboratory and field conditions for their insecticidal toxicity against RPM and other spider mites and insects. Abamectin is obtained from the fermentation caused by the soil micro-organism *Streptomyces avermitilis* Burg, and is considered the most efficient for controlling mites (Abd-Elhady & Abou-Elghar, 2013). It is a non-selective pesticide (acaricide) originally formulated as an emulsifiable concentrate and used as an insecticide, nematocide, and acaricide for agricultural utilization (Moreira et al., 2020; Bai & Ogbourne, 2016). Studies indicated that Abamectin is a powerful insecticide that poses high toxicity to mammals when used in large quantities and in high doses to control various pests (Abd-Elhady & Abou-Elghar, 2013; Bai & Ogbourne, 2016). However, in some cases, higher amounts of this acaricide are required to control RPM to cover all parts of the palm tree (Welbourn, 2006). This is because most of the pesticides are lost during the application, depending on the surrounding environment, resulting in degradation, evaporation, runoff, and leaching of pesticides, and approximately 0.1 % remains ultimately effective on the target pest (Zhao et al., 2017; Elabasy et al., 2020). Hence, modern nanotechnologies may be required to decrease the amounts and the environmental risk of pesticides while maintaining their effectiveness (Lee et al., 2016). The nanoemulsion technique is becoming increasingly popular in the pest management field since it is highly credible and effective for developing pesticides that

are less harmful, more effective, and more cost-effective than conventional pesticides (Lu et al., 2018; Elabasy et al., 2020; Mustafa & Hussein, 2020). The physical and chemical properties of nano-based pesticide formulations, such as high stability, decreased droplet size (20 –200 nm), high kinetic stability, and low viscosity, have led to enhancing the characteristics of the pesticide, such as distribution, targeting delivery, solubility, and stability (Debnath et al., 2012; Lu et al., 2018). Furthermore, these nanoemulsion properties, particularly the tiny particle size, reduce the spray solution used for pest control (Lee et al., 2016; Huang et al., 2018). At the same time, nanotechnology-based pesticide delivery systems improve adhesion to plant leaf surfaces, allowing active ingredients to be released and delivered more effectively (Scott et al., 2018).

Despite these unique features mentioned above, the nanoemulsion formulation of Abamectin has not been investigated yet. Therefore, the present study aims to prepare the nanoemulsion formulation of this acaricide by applying a low-energy method, in addition to improving the toxicity of Abamectin against the red palm mite (RPM), *R. indica* under laboratory conditions.

## Materials and Methods

### Chemicals

The Abamectin (1.8 % (w/v) active ingredient) emulsifiable concentrate (E.C.) pesticide was Manufactured by VAPCO CO. Ltd., Amman, Jordan. Tween 80 (T80) with 15 hydrophilic-lipophilic balance (HLB) and span 80 (S80) with 4.3 HLB were supplied by General Drugs House Co. Ltd., India. The white mineral (paraffin) oil (PO) was obtained from bioMérieux, France. Paraffin wax with a melting point of 60–62 °C was purchased from Biorex Biosciences Pvt. Ltd, India. Distilled water with neutral pH (7) was employed in the current study.

### Screening hydrophilic-lipophilic balance (HLB) value of the oil phase

The method of estimating the HLB values was adopted to find the proper value, which can be mixed with paraffin oil and water to prepare a nanoemulsion. Different ratios of S80 were blended with different amounts of T80 to prepare HLB ranging between 8 to 11.5. The HLB values were determined by a surfactant mixture that was calculated by equations 1 and 2:

**1 Equation.** 
$$\%a = \frac{100 (h - \text{span } 80 \text{ HLB } (4.3))}{\text{Tween } 80 \times 100 \text{ HLB} - \text{span } 80 \text{ HLB } (4.3)}$$

**Equation 2.** 
$$\% b = 100 - a$$

Where (h) is the required HLB values which were (8, 8.5, 9, 9.5, 10, 10.5, 11, 11.5), (a) is the ratio of T80, while b is the S80 ratio (Gadhav. 2014; Lu *et al.*, 2018). To find out the finest HLB values of the surfactant mixture that will be mixed with paraffin oil and water to acquire emulsion without separation, one gram of each HLB value, paraffin oil, and water was transferred into a 20 mL vial with a close-fitting cover. The mixture was blended using a vortex mixer (Model: Bionex KML-3000v, Korea) for one min. The mixtures were centrifuged (Model: MLW T30, Germany) at 3500 rpm for 30 min and stored for 24 h at room temperature. The phase separation was observed visually. The HLB values that achieved emulsion with one phase when mixed with water and paraffin oil were selected to construct a phase ternary diagram.

### **Ternary phase diagram construction**

The titration method was employed to form the ternary phase diagrams by preparing different mixtures paraffin oil and surfactant at ratios of 0:10, 1:9, 2:8, 3:7, 4:6, 5:5, 6:4, 7:3, 8:2, 9:1 and 10:0 (*w/w*) in 20 mL glass vial provided with an airtight lid. The water amount was modified and progressively added in a range of 5 % to 95 % of the whole volume of each mixture. Later, the mixtures were blended by a vortex mixer for one min .The mixtures were centrifuged at 3500 rpm for 30 min at  $27\pm 2$  °C, and the phase separation of each sample was observed visually. Based on the stability, transparency, and clarity of the samples, the ingredients phases were identified as anisotropic or isotropic. Chemix software (version 3.5), phase diagram plotter (UK) was used to draft and structure the ternary phase diagrams (Jiang *et al.*, 2012).

### **Selection of pre-formulation points from phase diagrams**

Two different pre-formulations were selected from the phase diagram. Various parameters were considered in choosing the pre-formulations, including the single-phase without gel, transparent appearance, and stability at room temperature. 35 % *w/w* Abamectin acaricide was added to the selected formulations and mixed using a vortexer for one min.

### **The kinetic and thermal stability tests**

The kinetic stability test was carried out by centrifuging 5 mL of each Abamectin nanoformulation at 3500 rpm for 30 min at  $27\pm 2$ °C (Mahmood *et al.*, 2020). While Abamectin nanoformulations thermostability tests were examined by storing 5 mL of each nanoformulation at  $27\pm 2$ °C for three months and oven condition at  $54\pm 2$ °C for two weeks, severally. After that, the phase separation was observed visually for all stability tests (Lee *et al.*, 2016). The

Abamectin nanoformulations, which passed the stability tests, were submitted to physicochemical characterizations and acaricidal toxicity tests.

### **Physicochemical characterizations of Abamectin nanoemulsion**

After being diluted with distilled water at a ratio of 1:20 w/w, the droplet size, polydispersity index (PDI), and zeta potential of formulations were measured at  $27\pm 2$  °C using photon correlation spectroscopy (Malvern Instrument, UK) with laser light scattering at 633 nm (Ullah et al., 2022). In addition, the ring method was followed to measure the surface tension of the Abamectin nanoemulsion formulation. The Tensiometer type KRUSS K6 (Krüss GmbH, Hamburg, Germany) with a 1.9 cm platinum ring was used to estimate the surface tension of the formulations at room temperature (Jiang *et al.*, 2011). Viscometer (Model: Brookfield; DV-II+Pro, UK) was utilized to evaluate the viscosity of formulations at room temperature. The viscosity value for each formulation was recorded after the sample equilibrium.

### **Droplet spreading test of normal and nanoemulsion formulations of Abamectin**

The hydrophobic surface (paraffinic wax) method, described by Mascarin *et al.*, (2014) with some modulation, was conducted to measure the spreading area of the normal and nanoemulsions Abamectin formulation. Twenty-five mL of melted paraffin wax at  $60\pm 2$  °C was added to Petri-dishes (60 ×15 mm) after hardening the paraffin wax. Six concentrations of each Abamectin formulation (25, 50, 100, 150, 200, and 250 mg/L) were prepared by diluting them with distilled water. Fifty µL of each concentration were transferred into Petri-dishes contain paraffin wax using micro-pipette (Eppendorf). Each treatment was replicated four times. The average of three diameters (mm) was measured randomly from each droplet after (1, 3, 6, 12, 15, and 18) hours of treatment by an electronic digital calliper. The spreading area of the droplets was calculated using equation 3.

$$\text{equation 3.} \quad \pi (r/2)^2$$

Where r is the diameter of the droplet.

### **Toxic activity of normal and nanoemulsion formulations of Abamectin against the red palm mite *R. indica***

The spraying method was applied to determine the acaricidal activity of the normal and nanoemulsion formulations of Abamectin against the RPM on the date palm leaflets. PRM-infested and uninfested date palm leaflets (*cv* Halawi) were collected from orchards in Abul-Khasib, Basra city, Iraq. The samples were placed in plastic containers and kept at  $27\pm 2$ °C and  $65\pm 5$ % RH for toxicity testing later. Seven concentrations of each Abamectin formulation type

(0, 25, 50, 100, 150, 200, and 250 mg/L) were prepared separately depending on the percentage of the active ingredient in each formulation by diluting with distilled water. Four discs with 2 cm diameters were taken from the uninfested palm leaflets for each treatment, these discs were sprayed in different concentrations using a small sprayer and left to dry for one hour at room temperature. After that, the discs were placed in Petri dishes (60 ×15 mm) containing wet cotton. Ten adults of RPM were transferred into each disc using a camel hair brush. The experiment was conducted in four replications. The mortality was observed after 6, 12, 15, 18, and 24 hours of spraying. The mite adults were considered dead if they did not respond or move when touched by a thin camel hairbrush (Dos Santos *et al.*, 2019). To obtain the median lethal concentration (LC<sub>50</sub>) and median lethal time (LT<sub>50</sub>), Probit regression analysis was conducted using Polo Plus-PC program Version 0.03 (LeOra Software). Values of LC<sub>50</sub> and LT<sub>50</sub> were considered non-significant if there was overlapping in confidence limit values. Furthermore, the toxicity index (TI) and toxicity increase percentage were calculated by equations 4 and 5.

**Equation 4.**  $(TI) = ((LC_{50} \text{ or } LT_{50} \text{ of normal or nano formulation}) / (LC_{50} \text{ or } LT_{50} \text{ of normal formulation}))$

**Equation 5.**  $\text{Toxicity increase \%} = (TI \text{ of normal formulation} - TI \text{ of nano formulation}) \times 100.$

When  $TI < 1$ , this means the nano formulation is highly toxic compared to the normal Abamectin formulation (Mossa *et al.*, 2019).

### Data analysis

The experiments were conducted in a completely randomized design with four replications. All data were analyzed using analysis of variance (ANOVA table). Tukey test was used to separate the means with significant differences at  $P < 0.05$ . The analysis was done using Statistical Analysis Software version 9.3

### Results

#### The required HLB values of nanoemulsion components

The results in table 1 show a discrepancy in the requirements for HLB values. HLB 9 and 11 combinations achieved homogeneity and one phase to the emulsion components, which were stable for 24 h under room temperature. While the other HLB values gave two phases when mixed with paraffin oil and water upon visual inspection after centrifugation or/and storage for 24 h at room temperature (Figure 1).

**Table 1. Determine the required HLB values of nanoemulsion components**

Nanoemulsion components			HLB Values							
Aqueous phase	Oil Phase	Surfactant	8	8.5	9	9.5	10	10.5	11	11.5
Water	PO	S80+T80	2ph*	2ph	1ph**	2ph	2ph	2ph	1ph	2ph

\* Two phases, \*\* one phase

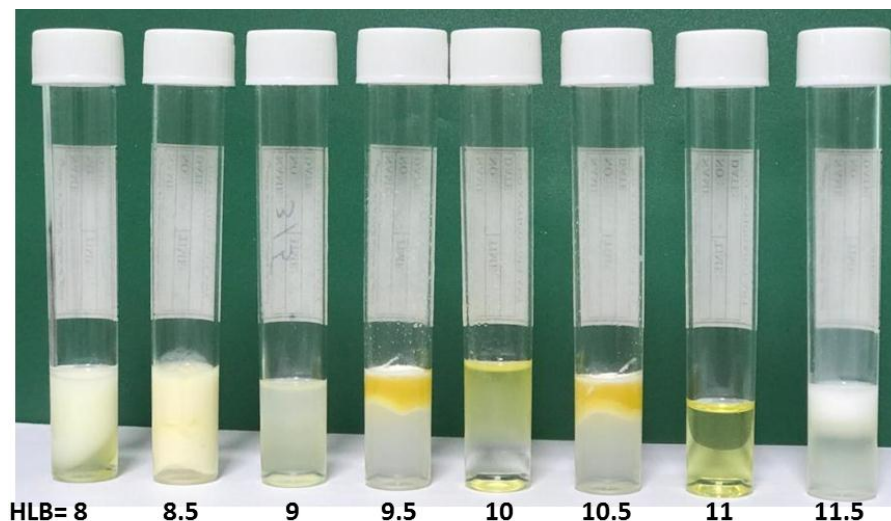


Figure 1. The appearance of the required HLB values of nanoemulsion components.

### Construction of the ternary phase diagrams

Two ternary phase diagrams were obtained from HLB 9 and 11 of S80+T80 surfactant mixture when mixed separately with PO as the oil phase and water as the aqueous phase (Figure 2). The ternary phase diagrams were employed to determine a nanoemulsion region (one phase). The behavior of the phase diagram of the ternary system that consisted of ratios of 9.62-48.18/ 21.10-46.90/ 26.17-53.16 of water/ surfactant mixture/ PO gave a 6 % transparent isotropic region. Furthermore, the ratios of 9.55-53.72/ 7.30-91.77/ 4.41-88.33 water/ surfactant mixture/ PO showed 39 % isotropic region. Nevertheless, 55 % two-phase region was formulated by the ratios of 0.00-95.05/ 0.00-37.55/ 0.00-98.38 of water/ surfactant mixture/ PO (Figure 2a).

On the other hand, the behavior of the ternary phase diagram system, which was formed by water as the aqueous phase, surfactant mixture at HLB 11, and PO as the oil phase, was somewhat different. It achieved 7 % transparent one phase region at ratios of 11.51-60.85/ 17.42-36-11/ 22.11-90.42, 41% one phase region at ratios of 9.87-91.33/ 3.87-80-77/ 1.38-91.60 and 52 % two-phase region at ratios of 0.00-91.35/ 0.00-20.55/ 0.00-100 water/ surfactant mixture/ PO (Figure 2b).

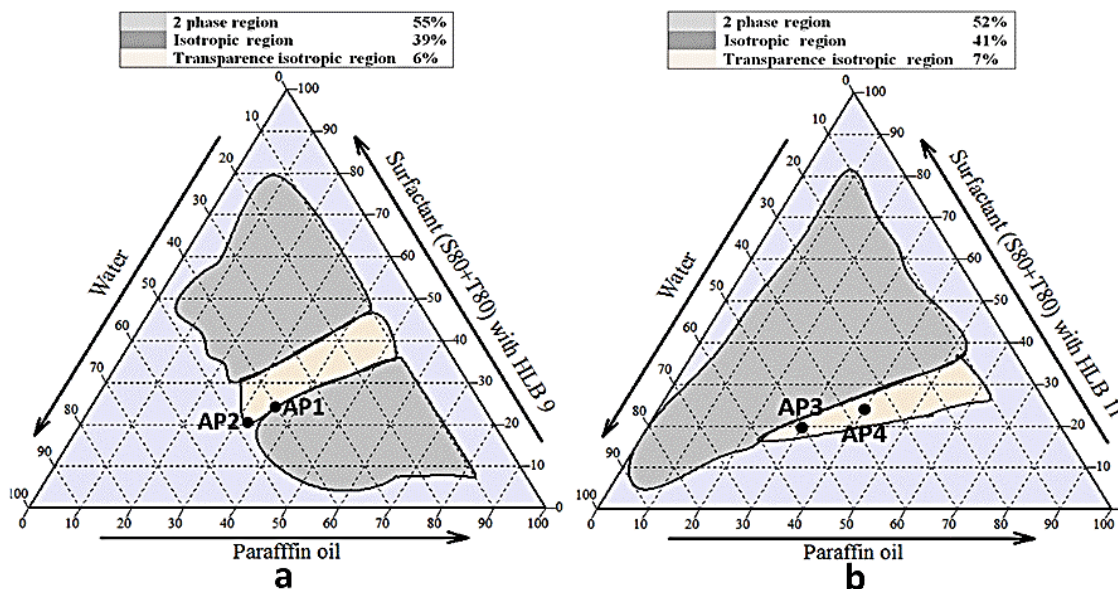


Figure 2. Ternary phase diagrams and the selected formulation points of water/ surfactant mixture at HLB 9 (a) and HLB 11(b)/ PO.

**Selection of pre-formulation points from ternary phase diagrams**

Two formulation points were selected from each phase diagram plot. The formulation points were chosen depending on three criteria, including the high ratio of water (40-50) % w/w, the low ratio of surfactant (20-25) % w/w, and the less ratio of oil (30-35) % w/w. to formulate an oil in water (O/W) nanoemulsion, 35 % of Abamectin were added of each selected formulation points. The selected formulations were coded as AP1, AP2, AP3, and AP4 (Figure 2 and Table 2).

**Table 2. Ingredient ratios of selected formulation points**

Formulation code	Ingredients ratio % (w/w)		
	Water	surfactant mixture	Paraffin oil (PO)
AP1	40	25	35
AP2	48	20	32
AP3	40	25	35
AP4	50	20	30

**The kinetic and thermal stability of the selected formulations**

The stability tests showed that AP1 and AP3 Abamectin nanoemulsion formulations gained high stability under all conditions of the stability tests without phase separation, creaming, colloid, and gel phase furthermore. Abamectin formulations AP2 and AP4 were stable under centrifuge

and storage at 27°C. However, these formulations suffered from phase separation or/and gel phase or/and creaming or/and colloid appearances during thermostability at 54°C. (Table 3, Figure 3).

**Table 3. The kinetic and thermal stability of abamectin nanoemulsion formulations**

Abamectin nanofrmulation code	Stability tests			Final result
	Kinetic	Thermostability tests		
		27 °C	54 °C	
AP1	√	√	√	Pass
AP2	√	√	×	Fail
AP3	√	√	√	Pass
AP4	√	√	×	Fail

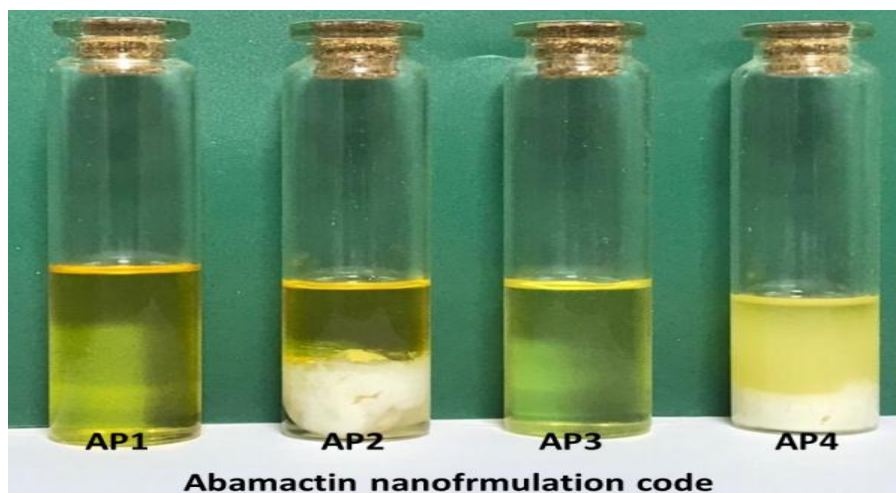


**Figure 3. The appearance of Abamectin nanoemulsion formulations after the kinetic and thermal stability testes**

#### Physicochemical characterizations of abamectin nanoemulsion

Table 4 summarizes the results of the physicochemical characterization of Abamectin nanoformulations. The results confirmed that all Abamectin formulation preparations were nanoemulsions with particle sizes ranging (from 137.45 to 54.20 nm). A good Polydispersive index (PdI) was obtained as Abamectin nanoformulation code AP1 recorded a higher deterioration of nanoparticles that was 0.25 compared with nanoformulation code AP3, which achieved 0.64. While the zeta potential values were fairly close (29.28 and 25.45 mV). The surface tension values of both Abamectin nanoformulation were somewhat similar with no significant differences ( $P < 0.05$ , Tukey). The viscosity results showed that the Abamectin

nanoformulation code AP1 had a higher viscosity than nanoformulation code AP3 that were 26.07 and 20.53 mPa s, respectively.

**Table 4. Abamectin physicochemical characterizations**

Abamectin Nanoformulation code	Particle size (d.nm)	Polydispersive index (PdI)	Zeta potential (mV)	Surface Tension (mN/m)	Viscosity (mPa s)
AP1	137.45±1.70a	0.25 ±0.01	29.28- ±0.78a	38.02±0.80a	26.07±0.64a
AP3	54.20 ±1.65b	0.64 ±0.05	25.45- ±0.24b	35.67±0.86a	20.53±0.93b

\* = similar letters in each column are not significant differences at  $P < 0.05$ . Tukey.

#### **The droplet spreading area of normal and nanoemulsion formulations of Abamectin**

Across all formulations tested, the spread area of droplets increased significantly as concentration and time after treatment increased for both normal and nanoemulsion formulations of Abamectin. However, droplet area decreased for all Abamectin formulations after 15 hours of treatment for all concentrations. Further, there were significant differences ( $P < 0.05$ ) in droplet spread area among the treatments (including formulation type, concentration, and time after treatment). The nanoformulation code AP3 achieved the largest spreading area followed by AP1 and normal formulation (N.ABA) of Abamectin. Further, 250 mg/L concentration recorded the largest spread area, followed by 200 > 150 > 100 > 50 > 25 mg/L for all Abamectin formulation types after 1, 3, 6, 12, 15 and 18 hours of treatment. Moreover, it was found that 15 hours after treatment of 25 and 250 mg/L concentration, 12 hours after treatment of 50 and 100 mg/L concentration, and 6 hours after treatment of 150 and 200 mg/L concentration recorded the largest spread area. In comparison, 1 hour after treatment of all concentrations recorded the smallest spread area compared with other times for all Abamectin formulation type. Furthermore, the results clarified that the largest spread area was 46.55 mm<sup>2</sup> after 15 hours, 45.65 mm<sup>2</sup> after 18 hours and 45.65 mm<sup>2</sup> after 12 hours of treatment at 250 mg/L of Abamectin nanoemulsion formulation code AP3. On the other hand, the normal Abamectin emulsion formulation (N.ABA) at 25 mg/L recorded the minimum droplet spreading area as 2.76 mm<sup>2</sup> after 18 hours of treatment (Figure 4).

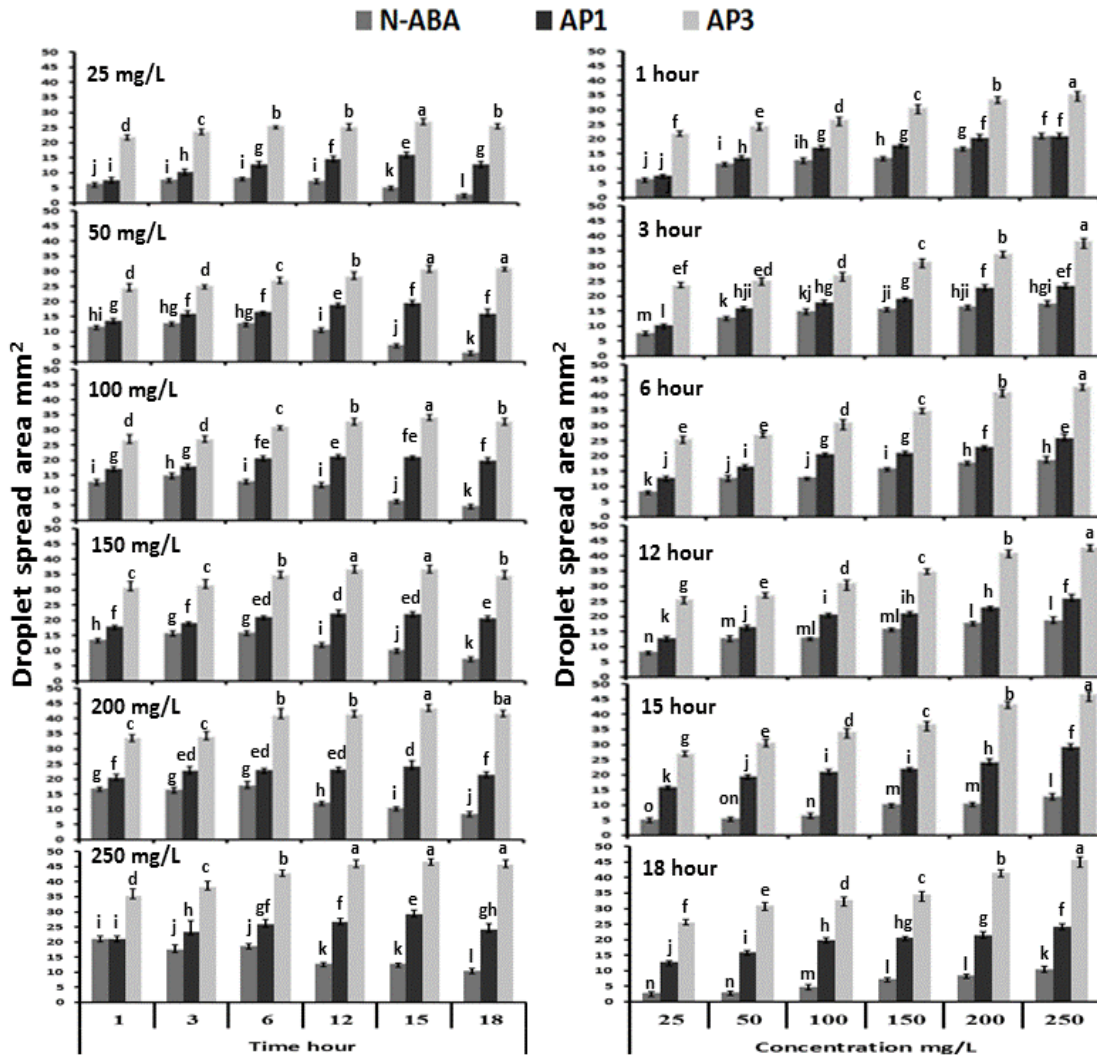


**Figure 4 Effect of concentration and time after treatment on droplet spreading area of the different Abamectin emulsion formulations**

\* = similar letters in each column are not significant differences at  $P < 0.05$ . Tukey.

**Toxic activity of normal and nanoemulsions formulation of Abamectin against RPM.**

The toxicity results revealed that the nanoemulsion formulations of Abamectin (AP1 and AP3) were more toxic against RPM compared with the normal formulation of Abamectin with significant differences (tables 5 and 6). Furthermore, the results confirmed that the acaricidal activity of all Abamectin formulations increased gradually with increasing concentration and time after treatment. The median lethal concentration ( $LC_{50}$ ) results indicated that the Abamectin nanoformulation AP3 significantly (no overlapping of confidence intervals) recorded high toxicity (lowest  $LC_{50}$ ) after 24 hours of treatment, followed by nanoformulation AP1 which were

32.77 and 38.67 mg/L, respectively. On the other hand, the normal Abamectin formulation recorded the lowest toxicity with the highest  $LC_{50}$  values followed by nanoformulation code AP3 and AP1, which were 1446.54, 1282.24 and 1222.94 mg/L, respectively, after 6 hours of treatment. Moreover, Abamectin's nanoemulsion showed higher toxicity against RPM than normal Abamectin emulsion after treatment. The toxicity index (TI) of nanoemulsion formulation of Abamectin code AP1 and AP3, depending on  $LC_{50}$  values, were 0.29 and 0.19 after 18 hours, 0.31 and 0.26 after 24 hours of treatment, respectively. In addition, the percentage of toxicity increase ranged (from 15.46 to 71.16) % and (from 11.36 to 80.83) % for Abamectin nanoemulsion formulation AP1 and AP3, respectively.

**Table 5. Normal and nanoemulsion formulation toxicity against the red palm mite *R. indica***

Abamectin formulation	Time hour	$LC_{50}$ mg/L	Confidence limit*		Slope SE.	Toxicity index TI	% of toxicity increase
			Lower	Upper			
Normal Emulsion	6	1446.54	641.08	18376.97	1.44±0.38	1.00	0.00
	12	749.24	405.65	3139.99	1.00±0.21	1.00	0.00
	18	383.02	254.18	854.21	1.01±0.19	1.00	0.00
	24	125.28	99.51	163.49	1.16±0.17	1.00	0.00
Nanoemulsion code AP1	6	1222.94	591.23	7912.64	1.23±0.29	0.85	15.46
	12	660.84	414.30	1713.34	1.43±0.27	0.88	11.80
	18	110.45	83.89	148.73	1.00±0.17	0.29	71.16
	24	38.67	26.68	49.85	1.36±0.18	0.31	69.13
Nanoemulsion code AP3	6	1282.24	585.70	10096.23	1.03±0.24	0.89	11.36
	12	281.26	199.76	519.39	1.09±0.19	0.43	62.46
	18	73.43	57.08	90.53	1.29±0.18	0.19	80.83
	24	32.77	23.83	41.17	1.72±0.20	0.26	73.84

The lowest  $LT_{50}$  values (highest toxicity) were obtained from Abamactine nanoformulation code AP3 followed by Abamectin nanoformulation code AP1 were 9.25 and 11.81 hours at 250 mg/L concentrations, respectively. Whilst the most extended  $LT_{50}$  values were 45.00, 30.91 and 28.40 hours at 25 mg/L concentration of normal formulation, nanoformulation code AP1 and nanoformulation code AP3 of Abamactin, respectively. Depending on the median lethal time

(LT<sub>50</sub>), the toxicity index was 0.61 at 50 mg/L of Abamectin nanoformulation code AP1 and 0.49 at 50 at 250 mg/L of Abamectin nanoformulation code AP3. Moreover, the percentage of toxicity increase ranged (from 28.63 to 38.87) % and ( from 31.31 to 50.97) % of Abamectin nanoemulsion formulation AP1 and AP3, respectively (Table 6).

**Table 6. LT<sub>50</sub> values and toxicity index (TI) of normal and nanoemulsion formulation of Abamectine against the red palm mite *R. indica***

Abamectin Formulation	Con. mg/L	LT <sub>50</sub>	Confidence limit*		Slope SE.	Toxicity index TI	% of toxicity increase
			Lower	Upper			
Normal Emulsion	25	45.0	32.74	104.00	2.97±0.72	1.00	0.00
	50	36.12	28.34	59.55	2.8-±0.50	1.00	0.00
	100	28.78	23.97	39.47	2.82±0.47	1.00	0.00
	150	25.43	21.22	34.31	2.41±0.40	1.00	0.00
	200	21.53	18.35	27.33	2.37±0.38	1.00	0.00
	250	18.72	16.33	22.39	2.57±0.37	1.00	0.00
Nanoemulsion code AP1	25	28.40	24.00	37.95	3.07±0.50	0.63	36.89
	50	22.08	19.36	26.61	3.04±0.43	0.61	38.87
	100	20.54	18.19	24.17	3.12±0.42	0.71	28.63
	150	17.59	15.56	20.40	2.84±0.37	0.69	30.83
	200	15.01	13.39	16.93	3.04±0.37	0.70	30.28
	250	11.81	10.09	13.59	3.55±0.38	0.63	36.91
Nanoemulsion code AP3	25	30.91	25.02	46.00	2.59±0.47	0.69	31.31
	50	17.71	15.85	20.20	3.19±0.37	0.49	50.97
	100	16.47	14.75	18.66	3.15±0.38	0.57	42.77
	150	14.56	12.99	16.40	3.04±0.37	0.57	42.74
	200	12.60	11.30	14.00	3.44±0.37	0.59	41.48
	250	9.25	8.22	10.21	4.01±0.40	0.49	50.59

## Discussion

The present study is the first report of applying Abamectin nanoemulsion as a nanoacaricide to control red palm mites. For that reason, in the current study, two O/W Abamectin nanoemulsions were successfully generated from paraffin oil as the oil phase and surfactant mixture (T80+S80) with HLB values 9 and 11 and water as the aqueous phase utilizing low energy method. Recently, using nanomaterials as pesticide delivery systems has attracted significant attention (Elabasy *et al.*, 2020; Mustafa & Hussein, 2020). Due to their low toxicity and effectiveness, oils like PO and nonionic surfactants like T80 and S80 have become common in the preparation of highly stable nanoemulsions by applying the low-energy method (Liu *et al.*, 2006; Kim *et al.*, 2014; Gupta *et al.*, 2017; Annisa *et al.*, 2020). The oil-in-water (O/W) nanoemulsion formulations are highly efficient and easy to apply in agricultural fields, especially in pest control (Scott *et al.*, 2018; Elabasy *et al.*, 2020). In fact, paraffin oil has low solubility in water, and adding nonionic surfactants (Tween 80 and Span80) can increase the solubility and distribution of oil. Therefore, the surfactant properties, such as chemical structure, viscosity, and HLB value, significantly influence nanoemulsion preparation (Annisa *et al.*, 2020). There is a specific HLB value for each surfactant and oil (oil phase). A stable nano-emulsification system can be achieved when the HLB of oil and water are compatible or reach the lowest interface tension between the aqueous phase and the oil phase (Syed & Peh, 2014). Ensuring a reasonable HLB value is critical for preparing a stable nanoemulsion formulation. Several studies indicated that the HLB values are one of the main determinants for forming a stable nanoemulsion (Komaiko & McClements, 2015; Gupta *et al.*, 2017; Algahtani *et al.*, 2022). Additionally, the appropriate mixture of surfactants with higher or lower HLB could prepare stable nanoemulsions, even when it is diluted, as a result of the ability of these mixtures of surfactants to reduce the surface tension, thus facilitating the dispersion process and forming an elastic film around the droplet (Lu *et al.*, 2018; Annisa *et al.*, 2020). Moreover, due to the broad distribution of chain lengths in nanoemulsions, they are usually formulated with a mixed surfactant to enhance stability (Lu *et al.*, 2018). Therefore, in the present study, the HLB value of the oily phase (paraffin oil) was experimentally determined by mixing the oil with a surfactant mixture of different HLB values. Choosing surfactants for nanoemulsion preparation depends on the HLB values that represent the strength and size of the hydrophilic and lipophilic parts in the surfactant molecule (Algahtani *et al.*, 2022). At 9 and 11 HLB values, a stable emulsion formed between paraffin as an oil phase and surfactant mixture due to PO's long carbon chain (C20-C60),

which requires a high HLB value (4-12) (Weerapol *et al.*, 2014; Hassan, 2018). In this regard, previous studies prepared a stable oil-in-water O/W nanoemulsion at 8-15 HLB value (Liu *et al.*, 2006; Jiang *et al.*, 2011; Agrawal *et al.*, 2017). A ternary phase diagram is a critical tool in choosing a highly stable nanoemulsion formulation, which is utilized to recognize the phase behavior when the ratio of emulsion ingredients (oil, surfactant, and water) starts changing gradually. In addition, the ternary phase diagrams present significant suggestions concerning the proportions of the formulation ingredients (Syed & Peh, 2014). Two ternary phase diagrams in the current study were obtained from paraffin oil and surfactant mixture at HLB 9 and 11 with water as the aqueous phase. Dual-acting surfactants (hydrophilic and lipophilic surfactants ) tend to demonstrate synergism that occurs due to the mutual electrostatic attraction between the hydrophilic group and the hydrophobic group, thus effectively reducing the interfacial tension at the water-oil interface. This leads to a highly stable nanoemulsion (Jiang *et al.*, 2011; Jiang *et al.*, 2012). The presence of surfactant (surfactant mixture) also contributes immensely to the construction of a stable colloidal dispersion of nanoemulsion through the synthesis of the surfactant film around emulsion particles and overcoming the repulsive forces of the aqueous and oil phases (Saengsorn & Jimtaisong, 2017; Algahtani *et al.*, 2022). It was observed larger O/W nanoemulsion area for the ternary phase diagram at HLB 11 compared with the ternary phase diagram at HLB 9. The reason is that the first combination (HLB 11) showed more compatibility with the other components compared to the second combination. In addition, the HLB 11 is more suitable for preparing O/W nanoemulsion because it is hydrophobic, which helps to disperse the oil phase in the aqueous phase and form a nanoemulsion compared with surfactant mixture at HLB 9 (Gupta *et al.*, 2017; Lu *et al.*, 2018). Jiang *et al.* (2011) reported that surfactants with HLB values over 10 could dissolve in water and adsorb on the droplet surface to form an oil-in-water (O/W) nanoemulsion. The results of the study showed that the formulations with a high ratio of surfactant (AP1 and AP3) possessed high kinetic and thermal stability. This is probably due to surfactant's role in increasing the stability of formulations by reducing the interfacial tension between water and oil, thereby dispersing oil into the water to form a stable emulsion. Thus, emulsions stay thermally and kinetically stable, distinguishing nanoemulsions (Debnath *et al.*, 2017; Lu *et al.*, 2018). Besides, the primary function of surfactants is to reduce free energy and to produce a mechanical barrier among formulation particles. Thus, surfactant agents minimize cloudiness and droplet size in the emulsion system (Fuentes *et al.*, 2021; Gupta *et al.*, 2017). Dual-acting surfactants (hydrophilic and lipophilic surfactants ) tend to demonstrate

synergism that occurs as a result of the mutual electrostatic attraction between the hydrophilic group and the hydrophobic group. Thus effectively reduces the interfacial tension at the water-oil interface, which leads to the formation of a highly stable nanoemulsion (Jiang *et al.*, 2011; Jiang *et al.*, 2012). The presence of surfactant (surfactant mixture) also contributes immensely to the construction of a stable colloidal dispersion of nanoemulsion through the synthesis of the surfactant film around emulsion particles and overcoming the repulsive forces of the aqueous and oil phases (Saengsorn & Jimtaisong, 2017; Algahtani *et al.*, 2022). In fact, the small amount of surfactant possibly loses these abilities at high temperatures and rapid movement of particles which leads to bias, collisions, and the convergence of the particles, causing non-stabilization of the emulsion system as a result of the increase in particle size (Jiang *et al.*, 2012). The result of physicochemical characterizations of Abamectin formulations showed that all formulations were good nano properties. However, these characterizations were strongly influenced by the HLB value of the surfactant mixture employed to prepare the nanoformulations. This may be because the HLB value of surfactant which was higher than 10 can form stable nanoemulsions with good qualities (Jiang *et al.*, 2011; Gupta *et al.*, 2017; Lu *et al.*, 2018). The results indicated that both AP1 and AP2 Abamectin nanoformulation particle sizes were nano range less than 200 nm. Moreover, there was an inverse relationship between the particle size and the HLB value of the surfactant mixture used in the preparation of the Abamectin nanoemulsion. This reflects the fact that the HLB value of surfactant plays an essential role in preparing a nanoemulsion. The supplement of a surfactant is crucial for the production of small-sized droplets as it reduces the interfacial tension, i.e., the surface energy per unit area between the oil and aqueous phases of the emulsion. Hence, surfactants are essential to formulate stable nanoemulsions (Debnath *et al.*, 2012; Jiang *et al.*, 2012; Lee *et al.*, 2016; Lu *et al.*, 2018). Gupta *et al.* (2017) reported that the low-energy method formulates nano droplet size by employing optimum surfactant to reduce the interfacial tension between the emulsion systems. The quality of the emulsification process depends on the values of polydispersity index (PdI). The low reflects that all the emulsions were nanoemulsion range, stable, and homogeneous distribution. PdI is the ratio of the standard deviation to the mean diameter of the droplet, which indicates the consistency of the formulation droplet size. A PdI value less than 0.2 shows homogenous properties of emulsion particles (Debnath *et al.*, 2012; Ullah *et al.*, 2022). However, PdI values less than 0.7 are considered acceptable for the formulation of stable nanoemulsions (Lee *et al.*, 2016). The differences in PdI may be attributed to differences in particle size, which have a significant effect on the PdI rate

(Ullah *et al.*, 2022). The zeta potential is a crucial measurement agent to explain the behavior and stability of different particles, representing the charge density on the surface of the emulsion particles. The formulation is considered stable if the zeta potential value is more than 25.00 mV (Lee *et al.*, 2016). All Abamectin nanoemulsions showed negative zeta potential values and more than 25.00 mV (29.28- to 25.45-). The increasing zeta potential leads to increasing the stability of the nanoemulsion by increasing the dispersion between the particles of the nanoemulsion, this produces emulsions that are stable against aggregation and separation (Lee *et al.*, 2016; Bot *et al.*, 2021). The high zeta potential values reflect the presence of repulsion between the particles of the emulsion, and this leads to a high stability of the nanoemulsion (Lee *et al.*, 2016). The difference in the zeta potential values of the emulsions prepared in the present study may be due to the different HLB values that significantly affect the value and type of zeta potential (Lee *et al.*, 2016). An inverse relationship between the zeta potential and particle size of Abamectin nanoemulsion indicates that the zeta potential increases of nanoemulsion when the particle size decreases and the surface area increases (Ullah *et al.*, 2022). The results showed a decrease in the surface tension values of the Abamectin nanoemulsions. The surfactants play a vital role in the melting of the oily phase in the water phase when preparing the formula, and this, in turn, reduces the surface tension value of the formulation (Siti *et al.*, 2012). Generally, the surfactant mixture reduces the surface tension through a synergistic action resulting from the electrostatic attraction between the hydrophilic and hydrophobic groups. This decreases the surface tension coefficient of the nanoemulsion (Jiang *et al.*, 2011). The results showed a decrease in the viscosity values of Abamectin nanoemulsion. The reduction in the viscosity values indicates an increase in the flow rate and a decrease in the dissociation rate of the nanoemulsion (Siti *et al.*, 2012). The viscosity of nanoemulsions decreases when the droplet size decreases. However, the nanoemulsion viscosity is related to the viscosity of nanoemulsion ingredients, ratios, and preparation methods (Liu *et al.*, 2006). In addition, the particle size significantly affects the viscosity of an emulsion. The small particle size is more dispersed in the emulsion, which leads to a lower viscosity value. The nanodroplet size reduces the cohesion force between the particles and, thus, decreases the viscosity of the emulsion (Liu *et al.*, 2006). Moreover, the viscosity is affected by the zeta potential value of an emulsion. When their actual volume fraction is less than their effective volume fraction, this leads to a significant decrease in the viscosity of the emulsion (Fuentes *et al.*, 2021). This explains why the viscosity value of the Abamectin nanoemulsion AP3 was less than Abamectin nanoemulsion AP1. The present study found that the Abamectin nanoemulsion

formulation with low viscosity, surface tension, and small particle size achieved the largest droplet spreading area. The variation in the spreading area of droplets may be due to their different physical properties, such as viscosity, surface tension, and particle size, which play a crucial role in droplet spreading. The decrease in particle size leads to an increase in the distribution area, a decrease in surface tension reduces adhesion, and a reduction of viscosity assists in increased runoff and flow (Siti *et al.*, 2012; Lu *et al.*, 2018). The addition of the surfactant materials reduces the surface tension and increases the droplet spread area. The droplet spread area expands by increasing the nanoemulsion concentrations, i.e surfactant concentration (Monadjemi *et al.*, 2011; Mascarin *et al.*, 2014). Therefore, it was observed that the spreading area of the treatments increased by increasing the concentration. The shrinkage of droplet areas after periods of treatment may be attributed to the occurrence of evaporation. In this regard, Yu *et al.* (2009) indicated that the evaporation coefficient of pesticides significantly impacts the distribution and spread of pesticides. The results showed that the nanoformulations of Abamectin showed large droplets spreading area compared to the normal formulation. This is a result of the unique properties of the nanoemulsions such as nanoparticle size, low viscosity, and low surface tension (Debnath *et al.*, 2017; Lu *et al.*, 2018). The toxicity results (LC<sub>50</sub>, LT<sub>50</sub>, TI, and % of toxicity) showed increases in the efficiency of the Abamectin nanoemulsion compared to the normal emulsion for all concentrations and periods. The results of previous studies were quite similar to the current study results that found an increase of the effectiveness of nanoemulsion formulation compared to non-formulated materials (normal formulation) (Mustafa & Hussein, 2020; Lee *et al.*, 2016; Lim *et al.*, 2012; Jiang *et al.*, 2011). Typically, the pesticidal activity of nanoparticles depends on the physiochemical properties of the nanoemulsion, especially the particle size. The emulsions with smaller particle sizes achieve high efficacy; therefore the Abamectin nanoformulation code AP3 achieved higher efficacy as an acaricide compared to the nanoformulation code AP1, this agrees with many previous studies (Lim *et al.*, 2012; Lee *et al.*, 2016). Furthermore, the nanoformulation system of pesticides enhances the activity by improving the controlled release, increasing solubility, and enhancing their distribution and penetration on the treated surfaces (Lee *et al.*, 2016; Huang *et al.*, 2017; Huang *et al.*, 2018). Furthermore, Abamectin nanoemulsions achieved higher mortality than normal Abamectin formulations on RPM. This is because of the penetration and spread of nanoemulsion into insect cuticles as a result of decreased particle size, resulting in higher toxicity (Mustafa and Hussein, 2020). The nanoformulations improve the delivery system of active ingredients to pests, which enhances the

performance of the pesticide. This is achieved through reduced surface tension, and a larger surface area (Jiang *et al.*, 2011). In addition, the study showed that the decrease in the surface tension increases the efficiency of the Abamectin nanoemulsion. The lower surface tension of nanoformulation may lead to adhesion of the active substance at a small angle of contact compared to the regular formulation. This allows an increase in the surface area of the modulus and increase penetration, thus increasing the effectiveness of the nanoformulation of the pesticide (Jiang *et al.*, 2012).

### **Conclusion**

The current study successfully formulated Abamectin as a nanoemulsion formulation utilizing low energy method by employing paraffin oil as an oil phase, (T80 + S80) as a nonionic surfactant, and water, as an aqueous phase. The nanoformulation of Abamectin possess high kinetic and thermal stability. Depending on the results of the study for a new nanoformulation of Abamectin that was nanoparticle size, lowest polydispersity, more inferior viscosity, less amount of optimum mixture of surfactant, and higher distribution of formulation particles. the normal Abamectin was improved as the O/W nanoemulsion formulation. Therefore the Abamectin nanoformulation has great potential to achieve higher PRM control efficiencies, thus reducing costs, delaying the development of insect resistance, and reducing side effects on the environment and human health.

### **References**

- Abd-Elhady, H. K., & Abou-Elghar, G. E. 2013. Abamectin induced biochemical and histopathological changes in the albino rat, *Rattus norvegicus*. *Journal of Plant Protection Research*,53(3), 263-270.
- Agrawal, N., Maddikeri, G. L., & Pandit, A. B. 2017. Sustained release formulations of citronella oil nanoemulsion using cavitation techniques. *Ultrasonics Sonochemistry*, 36, 367-374.
- Algahtani, M. S., Ahmad, M. Z., & Ahmad, J. 2022. Investigation of Factors Influencing Formation of Nanoemulsion by Spontaneous Emulsification: Impact on Droplet Size, Polydispersity Index, and Stability. *Bioengineering*, 9(8), 384.
- Annisa, R., Yuwono, M., & Hendradi, E. 2020. Design and optimization of Eleutherine palmifolia extract-loaded SNEDDS using HLB approach. *Journal of Research in Pharmacy*, 24(6), 943-951.
- Bai, S. H., & Ogbourne, S. 2016. Eco-toxicological effects of the avermectin family with a focus on Abamectin and ivermectin. *Chemosphere*, 154, 204-214.

- Bot, F., Cossuta, D., & O'Mahony, J. A. 2021. Inter-relationships between composition, physicochemical properties and functionality of lecithin ingredients. *Trends in Food Science & Technology*, 111, 261-270.
- Cocco, A., & Hoy, M. A. 2009. Feeding, reproduction, and development of the red palm mite (Acari: Tenuipalpidae) on selected palms and banana cultivars in quarantine. *Florida Entomologist*, 92(2), 276-291.
- Debnath, S., Kumar, G. V., & Satayanarayana, S. V. 2012. Design, Development and Evaluation of Novel Nanoemulsion of Terbinafine HCl. *Research Journal of Pharmacy and Technology*, 5(10), 7.
- Dos Santos, M. C., Teodoro, A. V., Menezes, M. S., Pinto-Zevallos, D. M., de Fátima Arrigoni-Blank, M., Oliveira, E. M. C., ... & Blank, A. F. 2019. Bioactivity of essential oil from *Lippia gracilis* Schauer against two major coconut pest mites and toxicity to a non-target predator. *Crop Protection*, 125, 104913.
- Elabasy, A., Shoaib, A., Waqas, M., Shi, Z., & Jiang, M. 2020. Cellulose nanocrystals loaded with thiamethoxam: fabrication, characterization, and evaluation of insecticidal activity against *Phenacoccus solenopsis* Tinsley (Hemiptera: Pseudococcidae). *Nanomaterials*, 10(4), 788.
- Fuentes, K., Matamala, C., Martínez, N., Zúñiga, R. N., & Troncoso, E. 2021. Comparative study of physicochemical properties of Nanoemulsions fabricated with natural and synthetic surfactants. *Processes*, 9(11), 2002.
- Gadhawe, A. (2014). Determination of hydrophilic-lipophilic balance value. *Int. J. Sci. Res*, 3(4), 573-575.
- Gupta, A., Badruddoza, A. Z. M., & Doyle, P. S. 2017. A general route for nanoemulsion synthesis using low-energy methods at constant temperature. *Langmuir*, 33(28), 7118-7123.
- Hassan, A. K. 2018. Assignment of Optimum Surfactants Blend and Right Oil Phase Concentration of Oil in Water Emulsion. *Indian Journal of Pharmaceutical Sciences*, 80(2), 334-341.
- Huang, B., Chen, F., Shen, Y., Qian, K., Wang, Y., Sun, C., ... & Cui, H. 2018. Advances in targeted pesticides with environmentally responsive controlled release by nanotechnology. *Nanomaterials*, 8(2), 102.

- Huang, Y., Hu, Q., Cui, G., Guo, X., Wei, B., Gan, C., ... & Cui, J. 2020. Release-controlled microcapsules of thiamethoxam encapsulated in beeswax and their application in field. *Journal of Environmental Science and Health, Part B*, 55(4), 342-354.
- Jiang, L. C., Basri, M., Omar, D., Rahman, M. B. A., Salleh, A. B., & Rahman, R. N. Z. R. A. 2011. Physicochemical Characterization of Nonionic Surfactants in oil-in-water (O/W) Nano-emulsions for New Pesticide Formulations. *International Journal of Applied*, 1(5), 131-142.
- Jiang, L. C., Basri, M., Omar, D., Rahman, M. B. A., Salleh, A. B., Rahman, R. N. Z. R. A., & Selamat, A. 2012. Green nanoemulsion intervention for water-soluble glyphosate isopropylamine (IPA) formulations in controlling *Eleusine indica* (*E. indica*). *Pesticide biochemistry and physiology*, 102(1), 19-29.
- Kim, E. H., & Cho, W. G. 2014. Stable liquid paraffin-in-water nanoemulsions prepared by phase inversion composition method. *Journal of the Society of Cosmetic Scientists of Korea*, 40(2), 133-139.
- Komaiko, J., & McClements, D. J. 2015. Low-energy formation of edible nanoemulsions by spontaneous emulsification: Factors influencing particle size. *Journal of food engineering*, 146, 122-128.
- Lee, K. W., bin Omar, D., bt Abdan, Khalina, & Wong, M. Y. 2016. Physicochemical characterization of nanoemulsion formulation of phenazine and their antifungal efficacy against *Ganoderma boninense* PER71 in vitro. *Research Journal Of Pharmaceutical Biological and Chemical Sciences*, 7(6), 3056-3066.
- Lim, C. J., Basri, M., Omar, D., Rahman, M. B. A., Salleh, A. B., & Rahman, R. N. Z. R. A. 2012. Physicochemical characterization and formation of glyphosate-laden nanoemulsion for herbicide formulation. *Industrial Crops and Products*, 36(1), 607-613.
- Liu, W., Sun, D., Li, C., Liu, Q., & Xu, J. 2006. Formation and stability of paraffin oil-in-water nanoemulsions prepared by the emulsion inversion point method. *Journal of colloid and interface science*, 303(2), 557-563.
- Lu, W. C., Huang, D. W., Wang, C. C., Yeh, C. H., Tsai, J. C., Huang, Y. T., & Li, P. H. 2018. Preparation, characterization, and antimicrobial activity of nanoemulsions incorporating citral essential oil. *Journal of food and drug analysis*, 26(1), 82-89.

- Mahmood, H. S., Alaayedi, M., Ghareeb, M. M., & ALI, M. M. M. 2020. The Enhancement Solubility of Oral Flurbiprofen by Using Nanoemulsion as Drug Delivery System. *International Journal of Pharmaceutical Research*, (1).
- Mascarin, G. M., Kobori, N. N., Quintela, E. D., Arthurs, S. P., & Júnior, Í. D. 2014. Toxicity of nonionic surfactants and interactions with fungal entomopathogens toward Bemisia tabaci biotype B. *BioControl*, 59(1), 111-123.
- Monadjemi, S., El Roz, M., Richard, C., & Ter Halle, A. 2011. Photoreduction of chlorothalonil fungicide on plant leaf models. *Environmental science & technology*, 45(22), 9582-9589.
- Moreira, R. A., de Araujo, G. S., Silva, A. R. R. G., Daam, M. A., Rocha, O., Soares, A. M., & Loureiro, S. (2020). Effects of Abamectin -based and difenoconazole-based formulations and their mixtures in Daphnia magna: a multiple endpoint approach. *Ecotoxicology*, 1-14.
- Mossa, A. T., Afia, S. I., Mohafrash, S. M., & Abou-Awad, B. A. 2019. Rosemary essential oil nanoemulsion, formulation, characterization and acaricidal activity against the two-spotted spider mite Tetranychus urticae Koch (Acari: Tetranychidae). *Journal of Plant Protection Research*, 59(1).
- Mustafa, I. F., & Hussein, M. Z. 2020. Synthesis and Technology of Nanoemulsion-Based Pesticide Formulation. *Nanomaterials*, 10(8), 1608.
- Nusantara, A., Trisyono, Y. A., Suputa, S., & Martono, E. 2017. Biology of Red Palm Mite, Raiiella indica, on different coconut varieties. *Jurnal Perlindungan Tanaman Indonesia*, 21(1), 23-29.
- Pena, J.E., J. Bruin, & M.W. Sabelis. 2012. Biology and Control of the Red Palm Mite, Raiiella indica: An Introduction. *Experimental and Applied Acarology* 57: 211–213.
- Saengsorn, K., & Jimtaisong, A. 2017. Determination of hydrophilic–lipophilic balance value and emulsion properties of sacha inchi oil. *Asian Pacific Journal of Tropical Biomedicine*, 7(12), 1092-1096.
- Scott, N. R., Chen, H., & Cui, H. 2018. Nanotechnology applications and implications of agrochemicals toward sustainable agriculture and food systems. *Journal of agricultural and food chemistry*, 66(26), 6451-6456.
- Siti, N. A., Dzulkefly, K. A., & Dzolkhifli, O. 2012. Evaluation of physicochemical characteristics of microemulsion formulation of rotenone and its insecticidal efficacy against Plutella xylostella L.(Lepidoptera: Plutellidae). *Journal of Food, Agriculture & Environment*, 10(3/4), 384-388.

- Song, Y., Wang, Q., Ying, Y., You, Z., Wang, S., Chun, J., ... & Wen, R. 2022. Droplet Spreading Characteristics on Ultra-Slippery Solid Hydrophilic Surfaces with Ultra-Low Contact Angle Hysteresis. *Coatings*, 12(6), 755.
- Syed, H. K., & Peh, K. K. 2014. Identification of phases of various oil, surfactant/co-surfactants and water system by ternary phase diagram. *Acta Pol Pharm*, 71(2), 301-9.
- Ullah, N., Amin, A., Alamoudi, R. A., Rasheed, S. A., Alamoudi, R. A., Nawaz, A., ... & Abbas, S. S. 2022. Fabrication and Optimization of Essential-Oil-Loaded Nanoemulsion Using Box–Behnken Design against *Staphylococcus aureus* and *Staphylococcus epidermidis* Isolated from Oral Cavity. *Pharmaceutics*, 14(8), 1640.
- Vásquez, C., Quiros De G, M., Aponte, O., & Sandoval, D. M. F. 2008. First report of *Raoiella indica* Hirst (Acari: Tenuipalpidae) in South America. *Neotropical Entomology*, 37(6), 739-740.
- Weerapol, Y., Limmatvapirat, S., Nunthanid, J., & Sriamornsak, P. 2014. Self-nanoemulsifying drug delivery system of nifedipine: impact of hydrophilic–lipophilic balance and molecular structure of mixed surfactants. *AAPS pharmscitech*, 15(2), 456-464.
- Welbourn, C. 2006. Red palm mite *Raoiella indica* Hirst (Acari: Tenuipalpidae). *Pest Alert. Florida Department of Agriculture & Consumer Services, Division of Plant Industry. Disponible en: Disponible en: <http://www.doacs.state.fl.us/pi/enpp/ento/r.indica.html>. [Fecha revisión: 27 enero 2015].*
- Yu, Y. A. N. G., Zhu, H., Frantz, J. M., Reding, M. E., Chan, K. C., & Ozkan, H. E. 2009. Evaporation and coverage area of pesticide droplets on hairy and waxy leaves. *biosystems engineering*, 104(3), 324-334.
- Zhao, X., Cui, H., Wang, Y., Sun, C., Cui, B., & Zeng, Z. 2017. Development strategies and prospects of nano-based smart pesticide formulation. *Journal of agricultural and food chemistry*, 66(26), 6504-6512.
- Zouba, A., & Raeesi, A. 2010. First report of *Raoiella indica* Hirst (Acari: Tenuipalpidae) in Tunisia. *Afr J Plant Sci Biotechnol*, 4(2), 100-101.

## تطوير وفعالية مبيد ابامكتين كمبيد حلم نانوي لمكافحة الحلمة الهندية الحمراء *Raoiella indicas* على نخيل التمر

ناصر حميد الدوسري ايهاب عبد الكريم النجم محمد عبد الباسط درويش

مركز ابحاث النخيل- جامعة البصرة -العراق

### الخلاصة

تعد الحلمة النخيل الهندية الحمراء *Raoiella indica* إحد الآفات الشائعة التي تصيب أشجار النخيل والتي قد تسبب أضراراً اقتصادية إذا تركت دون مكافحة. وقد استخدم مبيد الابامكتين على نطاق واسع في مكافحة هذه الآفة، إلا أن استخدامه بكميات كبيرة سبب أضراراً بيئية وصحية. نظراً للخصائص الفريدة لمبيدات النانوية، فقد تم تصميم الدراسة الحالية لإنشاء مستحلب نانوي مستقر للأبامكتين بتطبيق طرق منخفضة الطاقة، إذ حضر ثمانية تركيبات عن طريق مزج نسب مختلفة من Tween 80 و Span 80 التي تم خلطها مع زيت البارافين والماء و35% من مبيد الابامكتين، وبينت النتائج ان تركيبات اجازتا اختبارات الاستقرار الحركي والحراري تحت ظروف مختلفة من التخزين وكانت التركيبات عبارة عن مستحلب نانوي عند حجم جسيمات 54.20 و 137.45 نانومتر مع خصائص فيزيائية جيدة، وقد سجلت هذه التركيبات أكبر انتشار للقطيرات وحققت سمية عالية ضد افراد الحلمة الهندية مقارنة بمبيد أبامكتين التجاري (التقليدي). واعتمادا على هذه النتائج فان التركيبات النانوية للابامكتين توفر إمكانية زيادة كفاءة السيطرة على الحلمة النخيل الهندية الحمراء وبالتالي تقليل التكاليف وتؤخر ظهورصفة المقاومة وتقلل من الآثار الجانبية.

**الكلمات المفتاحية:** أبامكتين، حجم الجسيمات، السمية، منطقة الانتشار، HLB